



RAPID COMMUNICATION

A pipeline to characterize p53 effectors by integrative cistrome and transcriptome analysis in a genetically-defined organoid model



Tumor-protein 53 (p53) is a transcription factor (TF) encoded by *TP53* (*Trp53* in mice) and is a master regulator of tumor-suppressive programs¹. Importantly, *TP53* is the most frequently mutated gene in human cancer, and its loss of function contributes to tumor development, exemplified by variable p53 mutations detected in 50%–75% of pancreatic cancers.² From these perceptions, a number of targets transcribed by p53 that confer tumor suppression have been identified. Nevertheless, our understanding of how p53 prevents normal cells from initiating tumorigenesis is still incomplete. To complement this limitation, herein, we established a new approach to identify underlying effectors transcribed by p53 in normal physiology.

Our approach relies on a recently developed organoid culture enabling the expansion of epithelial cells derived from cancer tissues and genetically or histologically normal tissues.³ Among these culture systems, we chose a series of murine pancreatic organoids, which consists of four discrete stages of pancreatic cancer development: pancreatic epithelium that represents normality (N-organoid, derived from wild-type murine pancreas), intra-epithelial neoplasia (P-organoid), primary tumor (T-organoid), and metastasis (M-organoid). Except for N-organoids, the other three organoids are isolated from genetically-engineered mouse models for pancreatic cancer harboring different *Trp53* genotypes, namely, WT/WT (P), R172H/WT (T), and R172H/- (M).³ Therefore, we postulated that pancreatic organoid cultures with different genetic backgrounds of p53 would allow characterizing complete p53 cistrome.

Experimentally, we approached chromatin immunoprecipitation and sequencing (ChIP-seq) and RNA-sequencing

(RNA-seq) to reveal genes bound and transcribed by p53. We merged p53-bound ChIP-seq peaks identified from four types of pancreatic organoids if located within 1 bp overlap. Among these peaks, we considered 290 sites that showed confident levels of p53-binding signals on chromatin (normalized and averaged tag counts/peaks are greater than 20). From these p53-bound regions, we selected peaks annotated as promoters (± 2 kb from the transcription start site), which revealed 36 genes as candidates that are directly transcribed by wild-type p53. These 36 genes include 19 known participants in p53-downstream signaling (*i.e.*, *Cdkn1a*, *Ccng1*, *Bax*, and *Btg2*) (Fig. S1A). Meanwhile, whether other genes are directly regulated by p53 and involved in tumor suppression remained elusive (Table S1). Of note, we excluded *Pgk1* from further analysis with p53 occupancy at the promoter region in p53-mutated organoids (Fig. S1B). These approaches yielded 16 uncharacterized p53 target genes (Fig. 1A).

As anticipated, the promoter regions of 16 genes showed significantly lower p53-binding signals in M-organoids than the other three types of organoids, validating prior studies that the Arg-172 mutation impairs the DNA-binding affinity of p53 (Fig. 1B). Following these observations, RNA-seq analysis demonstrated that mRNA expression of established p53-targets, such as *Cdkn1a* and *Ccng1*, is significantly down-regulated in M-organoids, corroborating our cistrome-based strategy to reveal unknown p53 targets (Fig. S1C). Finally, we decided to focus on the four candidates that lost both p53 chromatin bindings and mRNA expression in M-organoids ($\log_2fc < -1$). These four candidates are α -glutamate cyclase (*Dgltcy*), epoxide-hydrolase-1 (*Ephx1*), F-box- and WD-repeat domain-containing-9 (*Fbxw9*), and Cluster-of-Differentiation-81 (*Cd81*) (Fig. 1C, D; Fig. S1D).

Peer review under responsibility of Chongqing Medical University.

<https://doi.org/10.1016/j.gendis.2023.03.009>

2352-3042/© 2023 The Authors. Publishing services by Elsevier B.V. on behalf of KeAi Communications Co., Ltd. This is an open access article under the CC BY-NC-ND license (<http://creativecommons.org/licenses/by-nc-nd/4.0/>).

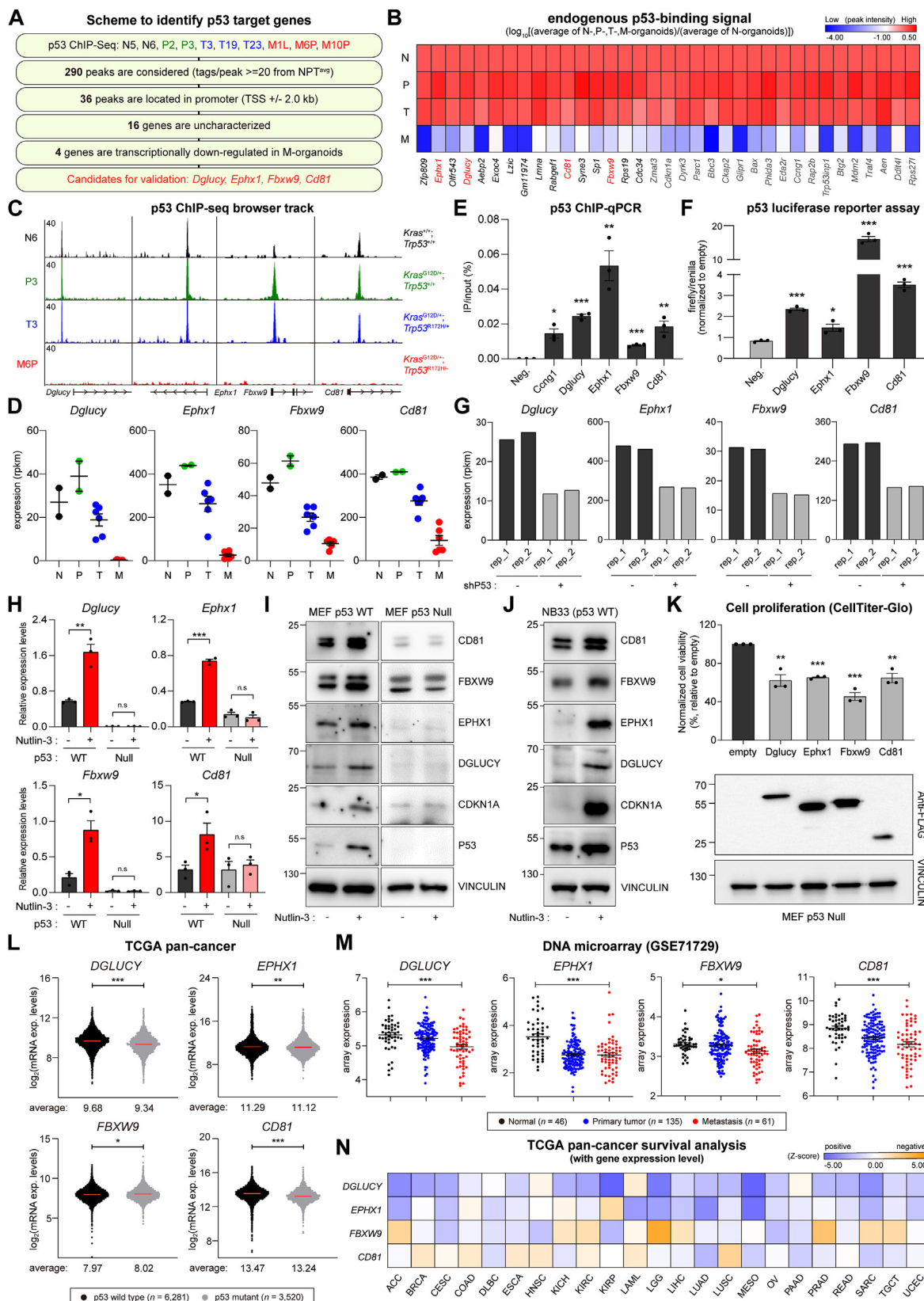


Figure 1 Identification and characterization of the physiologically relevant p53 target genes. **(A)** Schematic depiction of the process of nominating p53-target genes for characterization. **(B)** The heatmap showing endogenous p53-binding peak intensity of the indicated organoids (black = uncharacterized; gray = well-established targets; red = candidates for validation). **(C)** Representative ChIP-seq profiles of p53 in the indicated organoids at the *Dglucy* (Chr 12: 102,000,000–102,020,000), *Ephx1* (Chr 1:

p53 serves as a transcription factor by forming tetrameric complexes and binding selectively to its consensus motif, which consists of two repeats of the RRRCWWGYY decamer (R = A, G; W = A, T; Y = C, T).⁴ We used this information to determine whether *DgLucy*, *Ephx1*, *Fbxw9*, and *Cd81* could be directly targeted by p53. Notably, the areas near the TSSs of these genes that displayed the highest p53-binding affinities contained the core p53-binding sequence CWWG (Table S2). We validated the reliability of our ChIP-seq data by quantifying p53-occupied promoter regions of the four candidates via ChIP-qPCR analysis (Fig. 1E; Fig. S1E, F). To further test whether p53 binding sites at the promoters of candidates were responsive to p53, we designed reporter constructs by cloning predicted p53-binding sites into a promoter-less luciferase reporter plasmid (Fig. S1E, G). As a result, we observed the co-expression of p53 cDNA elevated luciferase signals of subcloned reporter constructs, indicating the promoter regions of four candidates possess p53-responsive elements (Fig. 1F). Together with these findings, we concluded that p53 is responsible for the direct induction of these four target genes under physiological conditions.

Next, to determine whether p53 is indispensable for the expression of the four genes, the P-organoids (which bear two copies of wild-type p53) were subjected to retroviral transduction with p53-targeting shRNA (shp53.1224), and confirmed efficient knockdown of p53 with a decrease in down-regulation of its targets (Fig. S1H). Notably, the p53 knockdown significantly suppressed the expression of all four target genes (Fig. 1G). As an orthogonal approach, fibroblast cultures with wild-type p53 (MEF or NIH/3T3) were incubated with Nutlin-3 for 24 h. The treatment of Nutlin-3 can potentiate the p53 pathway by impairing the interaction of p53 with MDM2.⁵ Quantitative reverse transcription PCR (RT-qPCR) and western blotting analysis showed that forced p53 stabilization was sufficient to up-regulate mRNA and protein levels of DGLUCY, EPHX1, FBXW9, and CD81 in MEF or murine pancreatic cancer cells with wild-type p53 (Fig. 1H–J; Fig. S1I, J). In contrast, we did not observe Nutlin-3 mediated induction of the four

genes in p53-deficient MEF cells. To further assess whether p53-dependent induction of the four genes confers anti-tumorigenic phenotypes, p53-deficient MEF cells were lentivirally transduced with the cDNA of the four genes. Compared to the empty vector control, stable expression of the four genes significantly reduced the proliferation rate of MEF cells (Fig. 1K). These results strongly indicate that p53-mediated direct transactivation of the four genes supports p53-dependent anti-tumorigenic phenotypes.

Next, to demonstrate the human relevance of our findings, we analyzed publicly available p53-ChIP-seq data from Nutlin-3-treated and untreated MCF7 cells, a human breast cancer cell line with wild-type p53. Consistent with our results from murine cultures, Nutlin-3 promoted p53 enrichment near the consensus p53-binding motifs in the promoter regions of the four genes (Fig. S1K). Moreover, Nutlin-3 mediated induction of the four genes in wild-type p53-containing U2OS, not in p53-deficient SAOS-2 osteosarcoma cells (Fig. S1L, M), supports p53-dependent induction of the four genes in the human settings. Finally, to extend the clinical relevance of these four genes in human cancer, we compared 33 tumor types profiled by The Cancer Genome Atlas (TCGA). We found that when stratified by p53 genotypes, tumors with wild-type p53 are associated with higher mRNA expression of targets than tumors bearing mutant p53 (Fig. 1L), which motivated us to examine human cancer. From the microarray-determined mRNA expression in normal pancreas and matched primary-metastatic pancreatic tumors, in particular, we found the progression of the pancreatic tumor was tightly associated with decreased mRNA expression of the four genes (Fig. 1M). Regarding post-diagnosis survival times, the analysis of the TCGA pan-cancer panel indicated that patients whose tumors expressed DGLUCY, EPHX1, FBXW9, or CD81 at lower levels tend to exhibit poorer prognostic outcomes than patients with higher expression levels (Fig. 1N). Nevertheless, the possibility of context-dependent tumor suppressive mechanisms remained to be explored (Fig. S1N).

In this work, we combined multiple approaches, including integrating p53 chromatin-binding sites with

182,925,000–182,935,000), *Fbxw9* (Chr 8: 87,584,000–87,590,000), and *Cd81* (Chr 7: 150,240,000–150,245,000) loci (from left to right). (D) mRNA expression of *DgLucy*, *Ephx1*, *Fbxw9*, and *Cd81* in murine pancreatic organoids. (E) ChIP-qPCR showed p53 enrichment (IP/input) at *Ccng1*, *DgLucy*, *Ephx1*, *Fbxw9*, and *Cd81* loci in NIH/3T3. (F) The bar graph showing relative luciferase activity driven by p53 in HEK-293 that transfected with wild-type p53 (or empty). pGL3-enhancer vectors were subcloned with p53-binding regions of *DgLucy*, *Ephx1*, *Fbxw9*, and *Cd81*. (G) mRNA expression of *DgLucy*, *Ephx1*, *Fbxw9*, and *Cd81* in P3 organoid with stable expression of shRenilla (–) or shP53.1224 (+). (H) Relative mRNA expression of *DgLucy*, *Ephx1*, *Fbxw9*, and *Cd81* in MEFs after 24-h treatment with DMSO (–) or 10- μ M Nutlin-3 (+). (I, J) Western blot analysis for DGLUCY, EPHX1, FBXW9, and CD81 proteins in (I) MEFs (p53 WT or Null) and (J) NB33 (p53 WT) after 24-h treatment with DMSO (–) or 10- μ M Nutlin-3 (+). (K) Luminescent-based cell viability assay and Western blot analysis of p53-deficient MEFs with stably expressed DGLUCY, EPHX1, FBXW9, and CD81. (L) mRNA expression of *DGLUCY*, *EPHX1*, *FBXW9*, and *CD81* in patients stratified according to the p53 status of their tumor tissues. The classified patient samples ($n = 9801$) were obtained from cBioPortal for cancer genomics. Medians are indicated by red lines. (M) Microarray-determined mRNA expression of *DGLUCY*, *EPHX1*, *FBXW9*, and *CD81* in normal pancreas, primary PDA tumors, and metastatic PDA tumors. (N) The heatmap showing patient survival rates associated with *DGLUCY*, *EPHX1*, *FBXW9*, and *CD81* expression. Z-scores were calculated by Cox proportional hazards models from tcga-survival (<https://tcga-survival.com/>). All relative mRNA expression levels were calculated with each expression level of *Tbp*. All error bars indicate mean \pm SEM. All *P*-values were determined by Student's *t*-test; **P* < 0.05, ***P* < 0.01, ****P* < 0.001.

transcriptome profiles, validating p53-dependent expression patterns with loss- and gain-of-function assays, and determining clinical relevance. From the identification to the comprehensive characterization of DGLUCY, EPHX1, FBXW9, and CD81 as functional p53 effector molecules, we propose the validity of utilizing organoid cultures for cis-trome analysis. Furthermore, our study warrants future research on determining the molecular and biochemical characteristics of DGLUCY, EPHX1, FBXW9, or CD81 in context-dependent tumor suppression via p53.

Author contributions

J-HS, H-RK, and J-SR conceived the study, designed and conducted the experiments, performed the data analyses, and wrote and edited the original draft. All authors have approved its submission to *Genes & Diseases*.

Conflict of interests

The authors declare no conflict of interests.

Funding

This study was supported by grants from the National Research Foundation of Korea (No. 2021R1A2C4001420 and 2020M3F7A1094089) to J-SR. Besides, J-HS, H-RK, and J-SR are supported by the Brain Korea 21 FOUR Program. The sponsors had no role in the study design; collection, analysis, or interpretation of data; writing the report; and the decision to submit the article for publication.

Appendix A. Supplementary data

Supplementary data to this article can be found online at <https://doi.org/10.1016/j.gendis.2023.03.009>.

References

1. Fischer M. Census and evaluation of p53 target genes. *Oncogene*. 2017;36(28):3943–3956.
2. Jaffee EM, Hruban RH, Canto M, et al. Focus on pancreas cancer. *Cancer Cell*. 2002;2(1):25–28.
3. Boj S, Hwang CI, Baker L, et al. Organoid models of human and mouse ductal pancreatic cancer. *Cell*. 2015;160(1–2):324–338.
4. el-Deiry WS, Kern SE, Pietenpol JA, et al. Definition of a consensus binding site for p53. *Nat Genet*. 1992;1(1):45–49.
5. Tovar C, Rosinski J, Filipovic Z, et al. Small-molecule MDM2 antagonists reveal aberrant p53 signaling in cancer: implications for therapy. *Proc Natl Acad Sci U S A*. 2006;103(6):1888–1893.

June-Ha Shin, Hwa-Ryeon Kim, Jae-Seok Roe*

Department of Biochemistry, College of Life Science and Biotechnology, Yonsei University, Seoul 120-749, Republic of Korea

*Corresponding author.

E-mail address: jroe@yonsei.ac.kr (J.-S. Roe)

7 December 2022

Available online 7 April 2023